Inverse-photoemission spectroscopy of the unreconstructed, ideally H-terminated Si(111) surface

S. Bouzidi, F. Coletti, and J. M. Debever
Groupe de Physique des Etats Condensés, Université Aix-Marseille II, Case 901, F-13288 Marseille CEDEX 9, France

P. A. Thiry
Laboratoire Interdisciplinaire de Spectroscopie Electronique, Facultés Universitaires Notre Dame de la Paix, B-5000 Namur, Belgium

P. Dumas
LASIR, 2 Rue Henri-Dunant, Thiais F 94320, France

Y. J. Chabal
AT&T Bell Laboratories, Murray Hill, New Jersey 07974
(Received 17 June 1991)

The chemically prepared H/Si(111)-(1×1) surface has been studied by **k**-resolved inverse-photoemission spectroscopy (KRIPES) along the two main directions ($\bar{\Gamma}\bar{K}$ and $\bar{\Gamma}\bar{M}$) of the surface Brillouin zone. Two conduction bands are evident at 2.6 and 4.0 eV at $\bar{\Gamma}$ and display some dispersion. A marked asymmetry is observed in their dispersion along the $\bar{M}'\bar{\Gamma}\bar{M}$ direction. This asymmetry is a manifestation of the different contributions of the eigenstates associated with $\mathbf{k}_{\parallel}$ and $-\mathbf{k}_{\parallel}$ to the KRIPES cross sections.

INTRODUCTION

The electronic structure of clean silicon surfaces has been studied extensively either by direct- or inverse-photoemission spectroscopies.[1] The situation is usually complex due to a variety of reconstructions, characteristic of clean semiconductor surfaces. The cleaved Si(111) surface, for instance, has a 2×1 reconstruction, made up of a π-bonded chain arrangement.[2] High-temperature thermal annealing converts this metastable structure into a *strong*, 7×7 reconstruction, involving surface adatoms, dimers, holes, and even a subsurface stacking fault.[3,4] These two surfaces are characterized by occupied and unoccupied *surface states*[5,6] that can usually be identified by exposing them to atomic hydrogen. This method is possible because the H atoms saturate the dangling bonds, quenching the surface states and inducing well-defined bonding states;[7] yet the higher-energy features, such as the antibonding states, do not significantly affect the bulk bands. Thus, the hydrogen-covered silicon surfaces provide a convenient means to study the *silicon* surface region. The main problem to obtain useful data is the atomic imperfection of the H-covered surfaces. The 7×7 surface is literally disrupted by atomic H exposure, exhibiting a disordered top layer.[8] The H-exposed 2×1 surface can be locally ordered into a 1×1 arrangement but its long-range order is perturbed by steps and defects, as evidenced by an inelastic He-atom scattering study.[9] As a result, the measured electronic structures of the H-covered Si(111) surfaces are rather featureless and difficult to interpret.

In contrast to the atomic H exposure of clean silicon surfaces, wet chemical etching of silicon[10,11] has recently been used to produce atomically flat, ideally H-terminated and *unreconstructed* Si(111) surfaces, with an unprecedented degree of perfection.[12,13] The quality of these surfaces has been characterized by vibrational spectroscopies, with the study of the Si—H stretching vibration by infrared absorption spectroscopy,[10,11,13] the study of silicon phonons by inelastic He-atom scattering[14] and the study of both the chemical nature of the surface and the rest of the vibrational manifold by electron-energy-loss spectroscopy (EELS);[15] and by scanning tunneling microscopy (STM).[12,16] As theoretically predicted,[17] the STM measurements confirm that there are no electronic states in the gap. The exceptionally high degree of electronic passivity of the H-terminated surfaces is revealed most accurately by surface-recombination velocity measurements,[18] showing that fewer than the equivalent of 10^8 electronically active states/cm^2 are present on the chemically prepared surfaces. Furthermore, the ideally H-terminated Si(111) surfaces are stable in deionized water and in purged environments and can be introduced into ultrahigh vacuum (UHV) by means of a load-lock system.[11]

In this paper, we report on a **k**-resolved inverse-photoemission spectroscopy (KRIPES) study of this H/Si(111)-(1×1) surface. The absence of surface states in the gap and the perfection of the surface make it possible to probe transitions from the bulk conduction bands without interference from surface states. In the present experimental conditions, the $\mathbf{k}_{\parallel}$ dispersion is measured on a Si($\bar{1}\,\bar{1}\,\bar{1}$) surface along the $\bar{\Gamma}\bar{M}$ and $\bar{\Gamma}\bar{K}$ directions of the *unreconstructed* silicon surface Brillouin zone (SBZ). A marked asymmetry is observed in the dispersion curve along $\bar{\Gamma}\bar{M}$ when the two azimuths [$\bar{1}\,\bar{1}$2] (i.e., $\bar{\Gamma}\bar{M}$) and [1 1 $\bar{2}$] (defined as $\bar{\Gamma}\bar{M}'$) are investigated. It is interesting to note that a definite asymmetry has also been measured by

photoemission for the filled valence states of the As-terminated Si(111) surface.[19] As for the As/Si(111)-(1×1) surface, the perfection of the chemically prepared H/Si(111)-(1×1) surface makes possible the observation of the details of bulk band asymmetry. For both surfaces, this asymmetry is explained by the fact that states with **k** and states with $-\mathbf{k}$ can contribute differently to the inverse-photoemission cross section. Thus, bands that are visible along $\bar{\Gamma}\bar{M}$ can be invisible along $\bar{\Gamma}\bar{M}'$, and vice versa.

EXPERIMENT

The KRIPES experiments are performed in an UHV chamber (base pressure $\sim 7\times 10^{-11}$ Torr), pumped by a 200-l/s ion pump and a liquid-N_2-cooled Ti sublimation pump, and equipped with low-energy electron diffraction (LEED) and Auger electron spectroscopy (AES) capabilities. A collimated beam of low-kinetic-energy (7–13-eV) electrons (angular divergence $\leq 3°$, i.e., $\Delta k_{\parallel} < 0.1$ Å^{-1}) originates from an electron gun with a BaO cathode. In order to avoid contamination and radiation damage, the average target current is limited to about 1 μA, and the sample orientation is checked with LEED, *only* at the very end of the KRIPES experiments. Note, however, that the total electron dose received by the sample during the measurements is small (10^{20} e^-/cm^2) so that the hydrogen desorption is negligible ($< 10^{-2}$ monolayer).[16]

For a given sample orientation, the dispersion within the surface Brillouin zone (SBZ) is investigated by rotating the electron gun, on either side of the sample normal, in a vertical plane perpendicular to the sample (i.e., by varying the polar angle θ). The sample can also be rotated about its vertical axis (angle ϕ), thus making it possible to measure the dispersion in the horizontal plane. Two orthogonal directions can therefore be probed during the same set of experiments (fixed electron gun rotating sample and vice versa). When possible, the configuration with the sample kept in place and the gun rotating is preferred, because it does not affect the focusing conditions of the mirror. To improve the angular precision, important for these measurements, the sample normal is first determined by measuring the target current: an extremum in the target current occurs when the incident electron beam is exactly normal. This technique gives a precision of $\pm 0.5°$. The sample is then rotated with a precision of $\pm 0.5°$. The exact azimuthal orientation of the sample is also determined by the Laue diffraction method.

The uv photons emitted by the sample are focused onto the detector by an elliptical mirror with 1 rad angular acceptance. The Geiger-Müller detector, filled with a helium-iodine mixture and sealed with a SrF_2 window, operates at an isochromat energy of 9.5 eV. The overall energy resolution, including the performance of the detector and the electron gun, is determined to be 0.35 eV by measuring the cutoff of the emission from a tantalum foil. The position of both this Ta foil and the sample can be rapidly exchanged, so that E_F is calibrated accurately for each spectrum.

The silicon substrates (8×15 mm^2) are n-type doped ($\rho \sim 120$ Ω cm). After degreasing in trichloroethylene, acetone, and methyl alcohol, the samples are cleaned in a solution of NH_4OH:H_2O_2:H_2O (1:1:4) at 80 °C for 10 min. They are then oxidized and etched twice, using a Shiraki solution and buffered HF, respectively.[20] After a third oxidation step in a solution of HCl:H_2O_2:H_2O (1:1:4) at 80° C for 10 min, the final etching step is performed in an ammonium fluoride solution (40% NH_4F, pH=7.8) during $6\frac{1}{2}$ min at room temperature. It should be emphasized that, between each step, the samples are thoroughly rinsed in deionized water (18.2 MΩ cm), particularly *after* the last etching step in ammonium fluoride. The samples are then quickly introduced into the UHV chamber by means of a load-lock chamber and according to well-defined procedures.[11] KRIPE experiments are carried out on the samples *without any further* cleaning or annealing. The LEED patterns obtained after the full KRIPE measurements are very sharp with no detectable diffuse background.

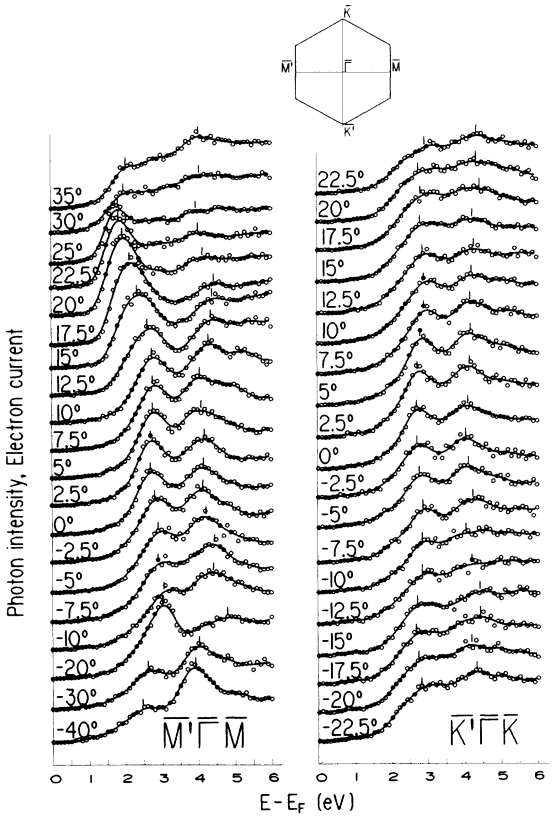

FIG. 1. **k**-resolved inverse-photoemission spectra of the H/Si(111)-(1×1) surface recorded at $h\nu = 9.5$ eV as a function of polar angle θ along the $\bar{M}'\bar{\Gamma}\bar{M}$ direction, by rotation of the electron gun (left panel), and as a function of the azimuthal angle ϕ along the $\bar{K}'\bar{\Gamma}\bar{K}$ direction, by rotation of the sample with the electron gun fixed (right panel). The vertical bars indicate the position of the main peaks, plotted in Fig. 2. Also shown is the Si(111)-(1×1) surface Brillouin zone with the main directions of analysis.

RESULTS

Before presenting the data, it is worth emphasizing that this is believed to be the first surface yielding KRIPE spectra without any further cleaning or annealing in vacuum. Inverse photoemission is extremely sensitive to the quality of the surface; for instance, inert surfaces such as graphite or GaSe have never produced useful KRIPE spectra even if they are freshly cleaved in air prior to introduction and even though they yield sharp LEED patterns. This observation confirms once again[11–15] the high quality and stability of the H/Si(111)-(1×1) surfaces, as well as the correctness of the pumping-down procedures.[11]

Figure 1 shows two series of KRIPES data recorded along the $\bar{\Gamma}\bar{K}$ direction (right panel) and along the $\bar{\Gamma}\bar{M}$ direction (left panel) of the SBZ. The intensity of the spectra is normalized to the target current and the energies are referenced to the Fermi level. The directions $\bar{\Gamma}\bar{K}$ and $\bar{\Gamma}\bar{K}'$ are probed by a positive (anticlockwise rotation) and negative (clockwise rotation) variation of the polar angle θ, respectively, maintaining the azimuth at $\phi=0°$. The directions $\bar{\Gamma}\bar{M}$ and $\bar{\Gamma}\bar{M}'$ are probed by rotating the sample from $\phi=-40°$ to $\phi=+35°$, and keeping $\theta=0°$.

In both cases, the spectra are devoid of any surface-state contribution in the gap, confirming the STM findings.[16] The spectra measured along $\bar{\Gamma}\bar{K}$ and $\bar{\Gamma}\bar{K}'$ (Fig. 1, right panel) show two conduction-band peaks, located at 2.6 and 4.0 eV above E_F at $\bar{\Gamma}$. They exhibit a very slight dispersion (see upper panel of Fig. 2) and are globally symmetrical with respect to $\bar{\Gamma}$ ($\theta=0°$) as $\mathbf{k}_\parallel$ is varied. In contrast, the spectra taken along the $\bar{\Gamma}\bar{M}$ direction (Fig. 1, left panel) are characterized by two states with definite asymmetry. For instance, note a difference of more than 1 eV between the energy position of the main peak for $\phi=+20°$ and $\phi=-20°$ (see lower panel of Fig. 2).

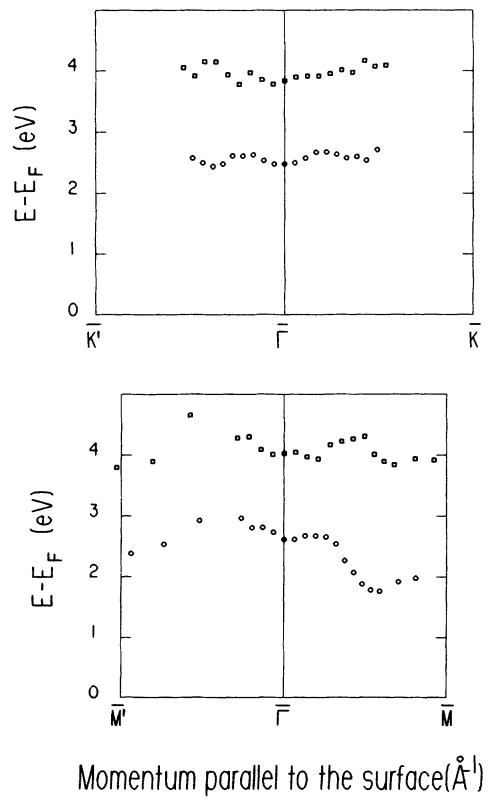

FIG. 2. Energy dispersion of conduction-band states along $\bar{K}'\bar{\Gamma}\bar{K}$ and $\bar{M}'\bar{\Gamma}\bar{M}$, determined from the data in Fig. 1.

DISCUSSION

Before discussing the asymmetry observed in our data, we first place our results in the context of previous work. The clean and H-covered cleaved Si(111)-(2×1) surface was studied using KRIPES by Perfetti, Nicholls, and Reihl.[6] In this study, the energy dispersion of an unoccupied surface-state band at ~1 eV above E_F was mapped out, from difference curves between the clean 2×1 and the H-covered 1×1 surfaces. Their results for the H/Si(111)-(1×1) surface along the $\bar{\Gamma}\bar{M}$ direction are in good agreement with ours as far as the dispersion of the lowest state is concerned. However, the dispersion was only studied for positive angles from 0° to 20°, so that the $\bar{\Gamma}\bar{M}'$ direction was not investigated.

At normal incidence ($\theta=0°, \phi=0°, \mathbf{k}_\parallel=0$ Å^{-1}), our spectra can be compared to another inverse-photoemission study of cleaved Si(111) by Straub, Ley, and Himpsel.[21] In that work, two states are measured at 2.4 and 4.15 eV above E_V which can be related to our states measured at 2.6 and 4 eV above E_F (see Fig. 2). The slight discrepancy is due to the weak energy dispersion of the Λ_1^c and Λ_3^c conduction bands along the ΓL direction. In addition, the energy dispersion of the Λ_1^c conduction band, within the range $0<\mathbf{k}_\parallel<0.4$ Å^{-1}, is in fairly good agreement with our corresponding results obtained on the H/Si(111)-(1×1) surface. This agreement suggests that measurements of the H/Si(111) surfaces probe states that are extended into the bulk (near-surface) region, and not just H-induced surface states. The H-antibonding states are in resonance with bulk conduction bands, i.e., there is a strong mixing, and the contribution from the bulk states may dominate.

An interesting result of this study is the marked asymmetry observed in the energy dispersion of the conduction-band states along $\bar{\Gamma}\bar{M}$ and $\bar{\Gamma}\bar{M}'$, i.e., along the two equivalent directions of the SBZ. It is therefore important to rule out any possible experimental artifact that could be responsible for such a behavior before discussing the results. For that purpose, the samples are mounted with their $\bar{\Gamma}\bar{M}$ axis oriented either vertical or horizontal, so that the $\bar{\Gamma}\bar{M}$ and $\bar{\Gamma}\bar{M}'$ directions are scanned either by rotation of the electron gun (θ) or of the target itself (ϕ), respectively. Both configurations, used for many different samples, give identical results, confirming the asymmetry. Note that no Laue diffraction data were available at the time of the KRIPES measurements and that the energy dependence of the LEED patterns was not used to distinguish $\bar{\Gamma}\bar{M}$ and $\bar{\Gamma}\bar{M}'$. As a result, the dispersion along one direction, e.g., $\bar{\Gamma}\bar{M}$, is obtained randomly for clockwise or anticlockwise rotations; and it is the asymmetry along the $\bar{M}\bar{\Gamma}\bar{M}'$ that makes it possible to index the samples and to orient properly the $\bar{K}\bar{\Gamma}\bar{K}'$ axis. The reproducibility of the data, including

the magnitude of the asymmetry, rules out possible artifacts and confirms that the asymmetry is an intrinsic property of the H/Si(111)-(1×1) surface.

This experimental observation of an asymmetry stresses a fact that has been recognized earlier in photoemission experiments[22] and inverse-photoemission experiments[23] of clean metal surfaces, namely that, although the eigenvalues have sixfold symmetry, the cross sections involving the corresponding eigenfunctions may not have sixfold symmetry because states with $\mathbf{k}_\parallel$ and $-\mathbf{k}_\parallel$ contribute differently. This can be seen in Fig. 3 where the position of Si atoms in the first four layers is shown, with different symbols for each layer. Consider the $\bar{\Gamma}\bar{K}$ direction first. The $[\bar{1}10]$ is one of the six azimuths corresponding to the $\bar{\Gamma}\bar{K}$ direction in the SBZ. Figure 3 shows that the atoms in the first four layers are symmetrically distributed with respect to the plane normal to the $[\bar{1}10]$ axis and containing the $[\bar{1}\,\bar{1}2]$ axis. Thus, the $\bar{\Gamma}\bar{K}'$ direction, which corresponds to the $[1\bar{1}0]$ azimuth, is strictly equivalent to $\bar{\Gamma}\bar{K}$ and symmetrical spectra are observed (Fig. 2, top panel).

This is not the case for the $\bar{\Gamma}\bar{M}$ direction, for which the $[\bar{1}\,\bar{1}2]$ is one of the six azimuths (see Fig. 3). It is clear that the plane normal to the $[\bar{1}\,\bar{1}2]$ axis and containing the $[\bar{1}10]$ axis is a mirror for the surface atoms only and *not for atoms of the second, third, and fourth layers.* As a result, the $\bar{\Gamma}\bar{M}'$ direction is not equivalent to the $\bar{\Gamma}\bar{M}$ direction, so that symmetrical spectra are not necessarily expected for inverse- or direct-photoemission spectroscopies which are sensitive to the first few silicon layers.

From the crystal symmetry point of view, one expects $E(\mathbf{k})$ to be equal to $E(-\mathbf{k})$ (time-reversal symmetry). In particular, the eigenvalues projected onto the (111) plane should display sixfold symmetry. The observed asymmetry simply shows that the eigenvectors that contribute to the inverse-photoemission intensity (the wave functions of the final states, more precisely) *are not probed with equal weight.* Some states may be invisible along $\mathbf{k}_\parallel$ and visible along $-\mathbf{k}_\parallel$. As a result, different eigenvalues contribute to the KRIPE spectrum, yielding an asymmetry.[22,23] The KRIPES measurements probe the joint density of empty conduction-band states separated by the isochromat energy of 9.5 eV and projected onto the (111) surface, as a function of $\mathbf{k}_\parallel$ only. There is an integration over $\mathbf{k}_\perp$, but the states with $\mathbf{k}_\perp<0$ (i.e., oriented towards the bulk) contribute differently to the KRIPES cross sections from those with $\mathbf{k}_\perp>0$ (i.e., oriented towards the vacuum). Figure 4 shows the cross section of the bulk Brillouin zone onto the plane containing $\mathbf{k}_\perp$ and $\mathbf{k}_\parallel$, along the $\bar{M}'\bar{\Gamma}\bar{M}$ direction (left) and along the $\bar{K}'\bar{\Gamma}\bar{K}$ direction (right). There is clearly an asymmetry between the projection along $\bar{\Gamma}\bar{M}$ and $\bar{\Gamma}\bar{M}'$, and no asymmetry for $\bar{\Gamma}\bar{K}$ and $\bar{\Gamma}\bar{K}'$.

It is interesting to compare our results to the early cal-

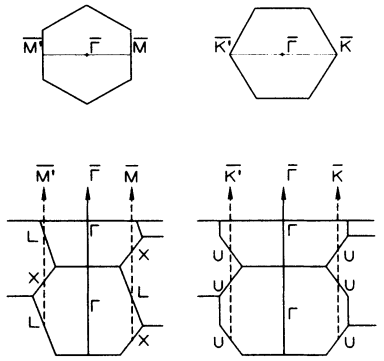

FIG. 4. Top: surface Brillouin zone of the Si(111)-(1×1). Bottom: corresponding cross sections along the $\bar{\Gamma}\bar{M}$ and $\bar{\Gamma}\bar{K}$ directions of the bulk Brillouin zone of the silicon truncated by the (111) plane.

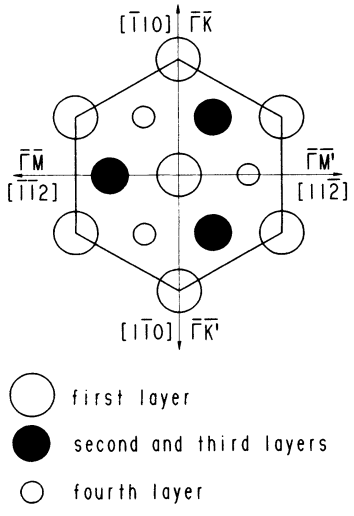

FIG. 3. Arrangement of the Si atoms below the (111) surface. Large open circles refer to the first layer, small open circles to the second and third layers, and solid circles to the fourth layer. The corresponding reciprocal-lattice directions are also indicated.

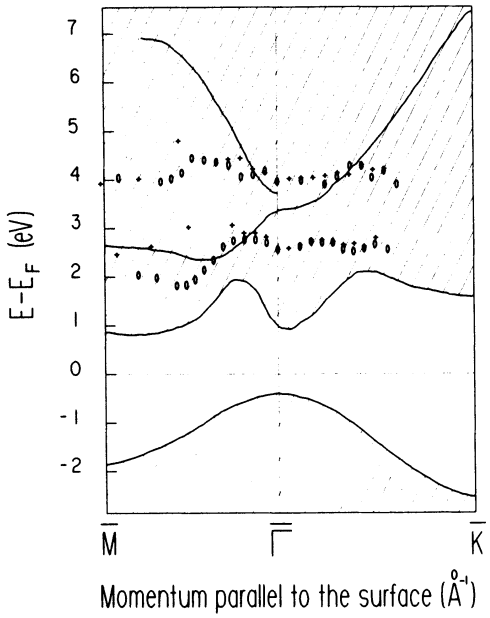

FIG. 5. Calculated surface-band structure (solid lines) for the H/Si(111)-(1×1) surface from Ref. 24. The experimental points are the result of the present work.

culations of Schlüter and Cohen[24] addressing the nature of conduction-band surface resonances for the Si(111) surfaces, including the H/Si(111)-(1×1). These calculations are based on self-consistent, semiempirical pseudopotentials and use the repeated slab configuration (with 12–14 layers each). They identify strong resonances involving the H-induced antibonding states and the bulk conduction-band states, summarized in Fig. 5 (solid lines). Note that the calculated energy bands were referred to the valence-band maximum and, according to Himpsel, Hollinger, and Pollack,[25] should be shifted downwards by 0.40 eV in order to be compared to our experimental results. Also note that, when the slab method is used as in Ref. 24, the resonances of both the front and back surfaces are averaged in order to eliminate possible artifacts arising from the finite slab size. The process of averaging washes out any asymmetry that may occur; in particular, differences in the dispersion of $\bar{\Gamma}\bar{M}$ and $\bar{\Gamma}\bar{M}'$ are averaged out. It is therefore satisfying to see that the average of our data for the lower branch along the $\bar{\Gamma}\bar{M}$ and $\bar{\Gamma}\bar{M}'$ directions can be accounted for by the theory along $\bar{\Gamma}\bar{M}$. This resonance at 2.5 eV has been identified as a Si *s*-like state present both at the surface and in the near surface region *of the unreconstructed* Si(111) surfaces.[24] Again, although this state could be associated to the H-antibonding state, its presence on both the H-terminated and clean Si(111) surfaces indicates that it involves mostly the Si states.

The agreement in the rest of the SBZ, along $\bar{\Gamma}\bar{K}$ for the 2.5-eV state and along $\bar{M}\bar{\Gamma}$ for the 4-eV state, is not as good. This is hardly surprising because the slab calculations with only 12–14 layers, as was only possible at the time, are not accurate to calculate bulk resonances. Nowadays, either Green-functions techniques[26] or better converged slab calculations[27] involving a larger number of layers should be used to unravel the nature of the resonances measured by inverse photoemission. It is clear, however, that experimental data obtained to date did not warrant sophisticated theoretical treatment because of the ambiguities arising due to surface imperfection and reconstruction and data quality such as resolution. The present system is clearly different, as evidenced by the ability to measure a dispersion asymmetry, and should motivate (when complementary photoemission data are available) detailed calculations addressing subtleties such as the dispersion asymmetry and the nature of the 4-eV bands.

CONCLUSIONS

The interest of the present study stems from the use of extremely homogeneous, *unreconstructed* Si(111) surfaces. These chemically prepared surfaces have been thoroughly characterized and provide an excellent model system to study the *bulk* silicon with techniques that are intrinsically surface sensitive (i.e., most electron and particle techniques). For instance, this inverse-photoemission study confirms that the H/Si(111)-(1×1) surface has no surface states in the gap and no distinct H-induced surface states in the conduction band. It is therefore "transparent" to the electrons so that the bulk can be studied. We can use our results to state that, since similar resonances are found on the clean 2×1 Si(111) surface, the 2×1 reconstruction does not affect the underlying bulk conduction-band states. This point can be further studied *in situ* because the hydrogen can be desorbed by electrons as recently shown by Becker *et al.*,[16] forming a 2×1 clean surface behind.

An interesting result of our study is the clear evidence for an asymmetry along the $\bar{M}'\bar{\Gamma}\bar{M}$ direction in the dispersion of the resonance observed around 2.5 eV above E_F. This asymmetry simply arises from the asymmetric arrangement of the second and fourth silicon layers, but has not been measured before because of surface reconstruction or poor surface quality. We feel that, when corresponding **k**-resolved photoemission data are available on this system, the experimental input will provide a stringent test for state-of-the-art Green's-function calculations,[26] and may even motivate sophisticated first-principles slab calculations.[27] Photoemission data should be particularly interesting in view of the available data on the As/Si(111)-(1×1) since any discrepancy may help highlight surface contributions to the spectra and/or differences in surface quality between the As- and H-terminated surfaces. For equal structural quality, important chemical differences exist. In particular, the As-terminated surface exhibits surface states in the gap or resonances close to the gap,[28] leaving the valence and conduction bands unperturbed away from the gap; in contrast, the H-terminated surface displays strong bonding states 5 and 7 eV below E_F (Ref. 17) and an antibonding resonance 4 eV above E_F.[24]

ACKNOWLEDGMENTS

The authors are grateful to C. Jourdan for the Laue diffraction measurements and to N. V. Smith, M. Schlüter, and M. S. Hybertsen for many useful discussions. The first three authors belong to the Groupe de Physique des Etats Condensés associated with the Centre National de la Recherche Scientifique.

[1]F. J. Himpsel, Surf. Sci. Rep. **12**, 1 (1990).
[2]K. C. Pandey, Phys. Rev. Lett. **47**, 1913 (1981).
[3]K. Takayanagi, Y. Tanishiro, M. Takahashi, and S. Takuhashi, J. Vac. Sci. Technol. A **3**, 1502 (1985).
[4]R. J. Hamers, R. M. Tromp, and J. E. Demuth, Phys. Rev. Lett. **56**, 1972 (1986).
[5]J. M. Nicholls and B. Reihl, Phys. Rev. B **36**, 8071 (1987).
[6]P. Perfetti, J. M. Nicholls, and B. Reihl, Phys. Rev. B **36**, 6160 (1987).
[7]T. Sakurai and H. D. Hagstrum, Phys. Rev. B **12**, 5349 (1975); H. Ibach and J. E. Rowe, Surf. Sci. **43**, 481 (1974); K. Fujiwara, Phys. Rev. B **24**, 2240 (1981).
[8]Y. J. Chabal, G. S. Higashi, and S. B. Christman, Phys. Rev. B **28**, 4472 (1983).

[9]U. Harten, J. P. Toennies, Ch. Wöll, L. Miglio, P. Ruggerone, L. Colombo, and G. Benedek, Phys. Rev. B **38**, 3305 (1988).
[10]G. S. Higashi, Y. J. Chabal, G. W. Trucks, and K. Raghavachari, Appl. Phys. Lett. **56**, 656 (1990).
[11]P. Dumas, Y. J. Chabal, and G. S. Higashi, Phys. Rev. Lett. **65**, 1124 (1990).
[12]G. S. Higashi, R. S. Becker, Y. J. Chabal, and A. J. Becker, Appl. Phys. Lett. **58**, 1656 (1991).
[13]P. Jakob, P. Dumas, and Y. J. Chabal, Appl. Phys. Lett. **59**, 2968 (1991).
[14]R. B. Doak, Y. J. Chabal, G. S. Higashi, and P. Dumas, J. Electron Spectrosc. Relat. Phenom. **54/55**, 291 (1990).
[15]P. Dumas and Y. J. Chabal, Chem. Phys. Lett. **181**, 537 (1991); Surf. Sci. (to be published).
[16]R. S. Becker, G.S. Higashi, Y. J. Chabal, and A. J. Becker, Phys. Rev. Lett. **65**, 1124 (1990).
[17]J. A. Appelbaum and D. R. Hamann, Phys. Rev. Lett. **34**, 806 (1975).
[18]E. Yablonovitch, D. L. Allara, C. C. Chang, T. Gmitter, and T. B. Bright, Phys. Rev. Lett. **57**, 249 (1986).
[19]R. I. G. Urhberg, R. D. Bringans, M. A. Olmstead, and R. Z. Bachrach, Phys. Rev. B **35**, 3945 (1987); see also details of the calculations to determine the electronic state dispersion in R. D. Bringans, R. I. G. Uhrberg, R. Z. Bachrach, and J. E. Northrup, Phys. Rev. Lett. **55**, 533 (1985); J. Vac. Sci. Technol. A **4**, 1380 (1986).
[20]W. Kern and D. A. Puotinen, RCA Rev. **31**, 187 (1970); W. Kern, Semicond. Int. **94**, (1984).
[21]D. Straub, L. Ley, and F. J. Himpsel, Phys. Rev. Lett. **54**, 142 (1985); Phys. Rev. B **33**, 2607 (1986).
[22]L. Ilver and P. O. Nilsson, Solid State Commun. **18**, 677 (1976).
[23]W. Altmann, V. Dose, and A. Goldmann, Z. Phys. B **65**, 171 (1986); R. F. Garrett and N. V. Smith, Phys. Rev. B **33**, 3740 (1986).
[24]M. Schlüter and M. L. Cohen, Phys. Rev. B **17**, 716 (1978).
[25]F. J. Himpsel, G. Hollinger, and R. A. Pollack, Phys. Rev. B **28**, 7014 (1983).
[26]See, for example, P. Krüger, M. Mazur, J. Pollmann, and G. Wolfgarten, Phys. Rev. Lett. **57**, 1468 (1986); P. Krüger and J. Pollmann, Phys. Rev. B **38**, 10 578 (1988).
[27]M. S. Hybertsen and S. G. Louie, Phys. Rev. B **38**, 4033 (1988).
[28]R. S. Becker, B. S. Swartzentruber, J. S. Vickers, M. S. Hybertsen, and S. G. Louie, Phys. Rev. Lett. **60**, 116 (1988).